Chapter 24

Numerical Simulation of Hydraulic Fracturing in Heterogeneous Rock: The Effect of Perforation Angles and Bedding Plane on Hydraulic Fractures Evolutions

Xiaoxi Men, Chun'an Tang, Shanyong Wang, Yongping Li, Tao Yang and Tianhui Ma

Additional information is available at the end of the chapter

http://dx.doi.org/10.5772/56012

Abstract

Considering the heterogeneity of rock, the hydraulic fracturing process of rock specimen due to internal hydraulic pressure was numerically simulated in a meso-scale by RFPA2D2.0 (Realistic Failure Process Analysis). The differences of perforation angle, bedding angle and bedding material of rock specimens are considered. The numerical results showed that the initiation and propagation of hydraulic fractures were controlled by both global pore pressure's distribution gradient and local pore pressure around the crack tip. Both the lateral compressive pressure ratio and the bedding angle could affect the evolution of the hydraulic fractures. The numerically simulated results were in agreement with the experimental results.

Keywords Hydraulic fracturing, heterogeneity, numerical simulation, fracture evolution

1. Introduction

Hydraulic fracturing is an important technology of production enhancement of oil and gas wells and intensified injection of wells. The first experimental hydraulic fracturing operation took place in the United States in 1947 in the Hugoton gas field in Grant County, Kansas, and after decades, the hydraulic fracturing technology has being widely used and become the dominant factor that determines the development plan of low permeability oilfield. In practical

applications, most of the hydraulic fracturing operations in the oil and gas fields are performed through casing, and, the regular or complex bedding structures likely exist in the rock mass formed in the course of rock formation and tectonic movement, so the research of the effect of perforation and bedding angle and modulus contrasts of rock and bedding in heterogeneous rocks under hydraulic fracturing is necessary. It can not only make fracturing decision-making more scientific, but reduce the fracturing cost and improve the fracturing efficiency, and has great theoretical significance and practical value on the perforation parameters optimization design and hydraulic fracturing construction of bedding rockmass.

At present, the perforation parameters are controllable which can be realized easily in practice. Since the hydraulic fracturing technology appeared, many experts have made various researches about the influence of perforation parameters on fracture evolutions under hydraulic fracturing. In [1], Daneshy et al. studied the hydraulic fracturing through perforation in 1973 and found that breakdown pressures of hydraulic fractures would decrease as the number of perforations increased, moreover, the existence of the casing and the perforations had little influence on the direction of the created fracture, which is perpendicular to the minimum principal stress. In [2], Weng et al. studied the hydraulic fracture initiation and propagation from deviated wellbores in 1993, investigated the interaction and link-up of the starter fractures initiated from perforations and the turning of the linked fracture and established a criterion that correlates fracture link-up to stresses and wellbore parameters. In [3], Zhang et al. used two-dimensional model to simulate the initiation and growth of hydraulic fractures in 2011 and developed a dimensionless parameter that is shown to characterise near-wellbore reorientation and curving of hydraulic fractures driven by viscous fluid. In [4], Zhang et al. employed three-dimensional finite element model together with the tensile criterion of rock materials in 2004, investigated that perforation density and perforation angle are the most important parameters controlling the formation fracturing pressure, but the influences of perforation diameter and perforation length are much slighter. In [5], Jiang et al. studied the fracture propagation mechanism of hydraulic fracturing through the experiment in 2009, and the results showed that the turning fracture can be generated by using oriented perforation fracturing technology, and with the increase of azimuth of oriented perforating, the breakdown pressure and turning distance are both growing.

Few studies have been carried on for fracture evolutions on heterogeneous rocks with different bedding angles under hydraulic fracturing at present stage. In [6], Bruno and Nakagawa studied fracture propagation path in non-uniform pore pressure field by test method in 1991, and proved that the fracture is influenced by both pore pressure magnitude on a local scale around the crack tip and the orientation and distribution of pore pressure gradient on a global scale. In [7], Li et al. simulated the experiment of hydraulic fracturing in non-uniform pore pressure field in 2005, and the results are well agreeable to that of Bruno and Nakagawa's experiments. In 2010, Abbass et al.'s study on Brazilian tensile text of sandstone in [8-9] showed that the breakdown pressure and fracture pattern are considerably affected by the bedding orientation and larger fracture length correlating with higher strength and applied energy.

http://dx.doi.org/10.5772/56012

In this paper, the effect of perforation and bedding angles and bedding materials on initiation pressure, breakdown pressure and hydraulic fractures evolutions of rock specimens under hydraulic fracturing is simulated and analyzed by using RFPA^{2D}(2.0)-Flow which adopts the finite element method and considers the heterogeneous characteristics of rock in meso-scale.

2. Introduction of RFPA^{2D}2.0-Flow

RFPA is a numerical experiment tool basing on the realistic failure process analysis method, which can simulate the gradual damage of materials. Its calculation method bases on finite element and statistical damage theory. RFPA considers both heterogeneity of materials and randomness of defect distribution, and puts the statistical distribution hypothesis of these material properties into the numerical calculation method (finite element method) to break the elements which satisfy the strength criterion. The material properties of each element follow Weibull distribution and are different from each other, and the element will fail if its stress reaches the failure strength, moreover, the number of fail elements will increase, which will be connected to each other and form fractures, as the load increases, so that the numerical simulation of heterogeneous material failure process can be realized. RFPA transforms the complex macroscopic nonlinear problem into simple mesoscopic linear problem by considering the heterogeneous characteristics of material and the complicated non-continuum mechanics problems into simple continuum mechanics problems by introducing the mathematics continuous and physical discontinuous concept, making the calculation results closer to the actual situation.

In mining and civil engineering projects, the re-distribution of the stress field during the excavation of tunnels and underground chambers leads to the formation of new fractures. The flow and transport behaviour within developing fractures are dramatically different from those in rocks with existing fractures under the same loading, therefore, the permeability of rocks changes dramatically in the process of damage evolution in fracture rocks. RFPA^{2D}2.0-Flow is the software considering the effects of the extension of existing fractures, the initiation of new fractures, the coupled effects of flow, stress and damage on the extension of existing/new fractures, and the permeability change due to damage evolution of the rocks, and is based on the theories of fluid-saturated porous media and damage mechanics. Flow-stress-damage (FSD) coupling model for heterogeneous rocks that takes into account the growth of existing fractures and the formation of new fractures is established herein. In [10-16], RFPA^{2D}2.0-Flow bases on the following five basic assumptions:

1. The fluid in the rock follows Biot consolidation theory;
2. Rock is the elastic brittle material with residual strength and the mechanical behaviour of loading and unloading process is in accordance with the elastic damage theory;
3. The maximum tensile strength criterion and Mohr Coulomb criterion are used as the damage threshold to judge whether the elements damage or not;

4. In elastic state, stress-permeability coefficient relationship of material is described by negative exponential function;

5. The mechanical parameters (such as uniaxial compressive strength f_c and elastic modulus E_c) of material at meso-scale (elements) are endowed by the following Weibull distribution:

$$\varphi(a) = \frac{m}{a_0}\left(\frac{a}{a_0}\right)^{m-1} e^{-\left(\frac{a}{a_0}\right)^m} \tag{1}$$

In this formula, a represents the mechanical property parameters of material (rock) elements at meso-scale; a_0 represents the statistical average of mechanical property parameters a; m is called homogeneity index, and higher m value means more homogeneity material; $\varphi(a)$ defines the statistical distribution density of mechanical property parameters a. Weibull's distribution for mechanical properties of materials with different homogeneity indexes m is shown in figure 1.

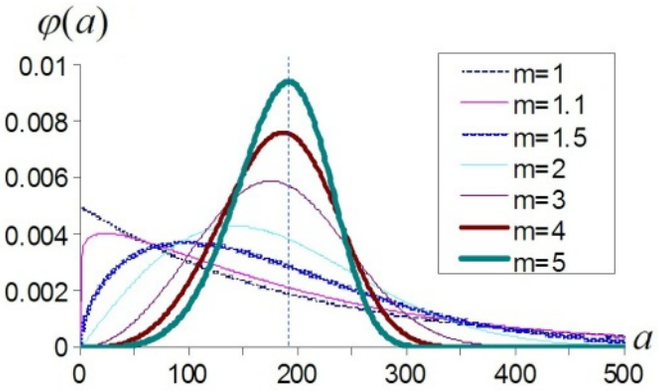

Figure 1. Weibull's distribution for mechanical properties of materials with different homogeneity indexes m

3. Model set

Numerical model is divided into three groups and each of them contains seven models, the fracturing process of rock specimens with different perforation angles, different bedding angles and different bedding materials under increasing hydraulic pressure and constant confining pressure are simulated. Perforation angle α is the angle between perforation and the maximum principal stress direction (horizontal direction), bedding angle α is the angle between bedding and the maximum principal stress direction (horizontal direction), and both of perforation and bedding angles chosen in the simulation are 0°, 15°, 30°, 45°, 60°, 75° and 90° respectively. The geometry of 2D rock model is 0.64m×0.64m and has been discretized into a 320×320(6400 elements) mesh, and the model is calculated by using plane strain. As shown

http://dx.doi.org/10.5772/56012

in figure 2, there is a well in the centre of model with radius 0.064m, two perforations approx 0.002m wide and 0.03m long cut into the well to provide initial direction for hydraulic fracture. Casing is in the non perforation area of the well with its strength and stiffness higher and permeability less than rock, so the initiation of fracture only occurs on perforation tip, which is in line with the actual engineering situation. As shown in figure 3, the well's radius is 0.032m and the space of two adjacent parallel beddings 0.04m. In figure 2 and figure 3, the confining pressure of the modelσ_H (in horizontal direction) andσ_h (in vertical direction)are 15MPa and 10MPa respectively with the initial pressure of 12MPa applied in the well and an incremental pressure of 0.1MPa maintained. The mechanical parameters of rock and bedding materials adopted in this simulation are listed in table 1 and table 2. The change of the values of elastic modulus and uniaxial compressive strength of bedding material are listed in table 3, and the value in brackets refers to the ratio of bedding and rock material. Moreover, the bedding angle of seven different bedding materials models is 60° with other mechanical parameters are in line with table 2.

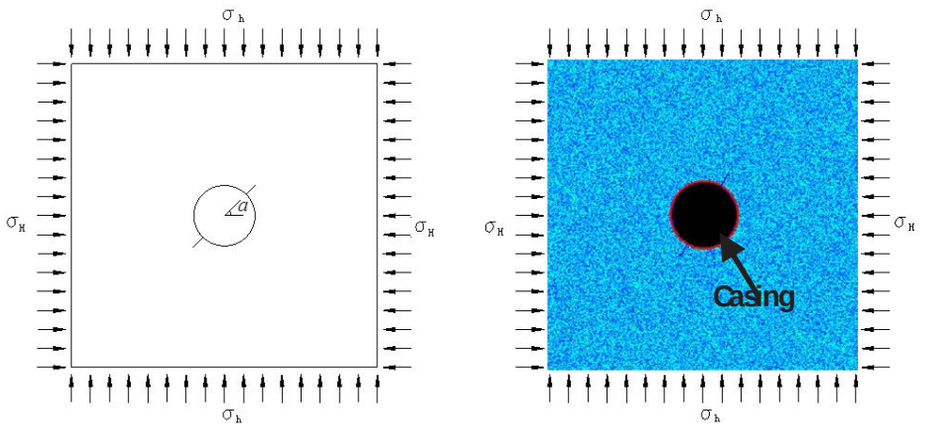

Figure 2. Schematic diagram and RFPA model diagram

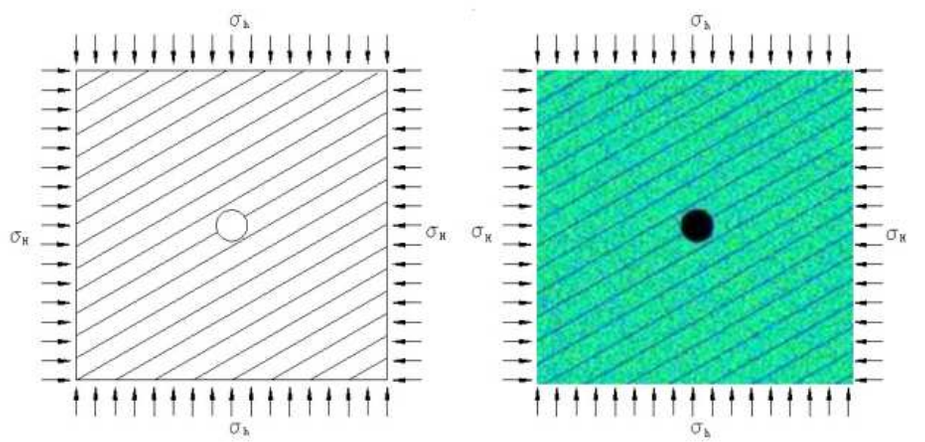

Figure 3. Figure 3 Schematic diagram and RFPA model diagram

Parameter	Symbol	Value
Homogeneity index	m	2
Elastic modulus	E_c	30 GPa
Poisson's ratio	μ	0.25
Internal friction angle	ϕ	37
Uniaxial compressive strength	f_c	200 MPa
Coefficient of permeability	K	0.000864 m/d

Table 1. Rock material mechanical parameter

Parameter	Symbol	Value
Homogeneity index	m	2
Elastic modulus	E_c	3.0 GPa
Poisson's ratio	μ	0.25
Internal friction angle	ϕ	37
Uniaxial compressive strength	f_c	20 MPa
Coefficient of permeability	K	0.00864 m/d

Table 2. Bedding material mechanical parameter

Rock material		Bedding material	
Elastic modulus (E_c)	**Uniaxial compressive strength (f_c)**	**Elastic modulus (E_c)**	**Uniaxial compressive strength (f_c)**
30GPa	200MPa	3.0GPa(1/10)	200MPa(1)
30GPa	200MPa	1.5GPa(1/20)	200MPa(1)
30GPa	200MPa	0.5GPa(1/60)	200MPa(1)
30GPa	200MPa	30GPa(1)	20MPa(1/10)
30GPa	200MPa	30GPa(1)	10MPa(1/20)
30GPa	200MPa	30GPa(1)	3.33MPa(1/60)
30GPa	200MPa	3.0GPa(1/10)	20MPa(1/10)

Table 3. Change of elastic modulus and uniaxial compressive strength values of bedding material

http://dx.doi.org/10.5772/56012

4. Simulation results

4.1. The effect of perforation angles

The initiation pressure, the breakdown pressure and the fracture evolution of seven rock specimens with different perforation angles under constant confining pressure and increasing hydraulic pressure are simulated. The results reflect the damage evolution process of rock specimen, which causes the macroscopic damage by microscopic under hydraulic fracturing and is consistent with the experimental result in [4]. Pore pressure and the minimum principal stress distribution of specimens with different perforation angles which achieved by numerical simulation are shown from figure 4 to figure 10. The comparison of the numerical simulation result and the experimental result which has the same perforation angle (60°) and under the same ground stress difference (5MPa) is shown in figure 11, and the values of the initiation and the breakdown pressure are shown in figure 12.

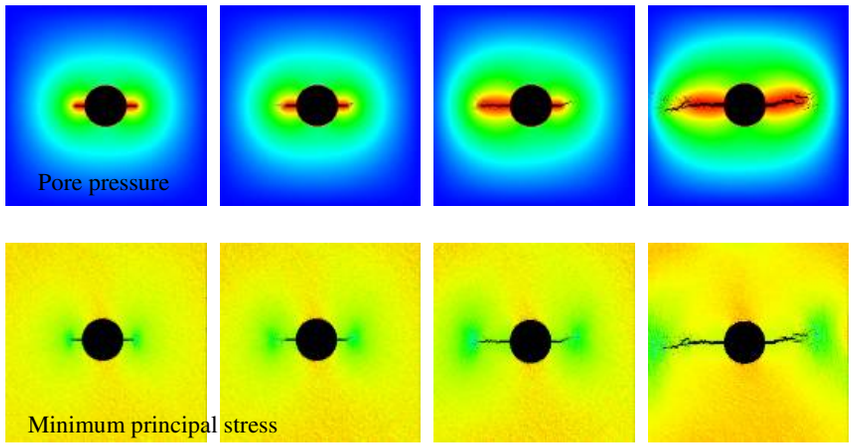

Figure 4. Pore pressure and the minimum principal stress distribution in fracture evolution process (0°)

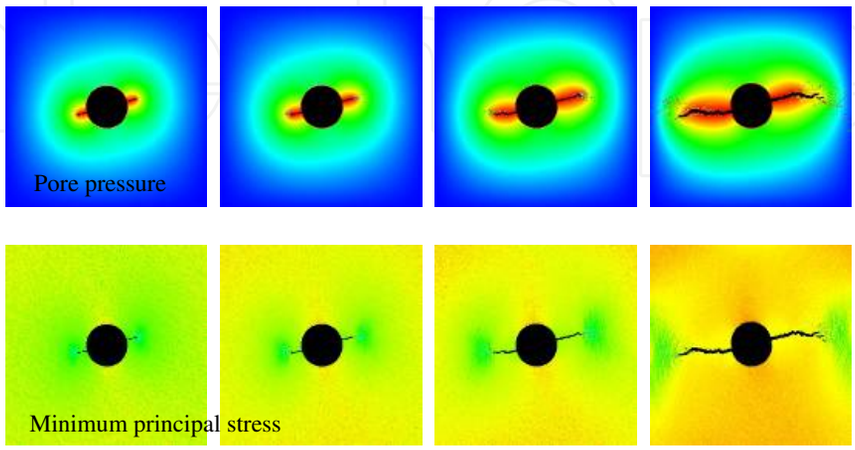

Figure 5. Pore pressure and the minimum principal stress distribution in fracture evolution process (15°)

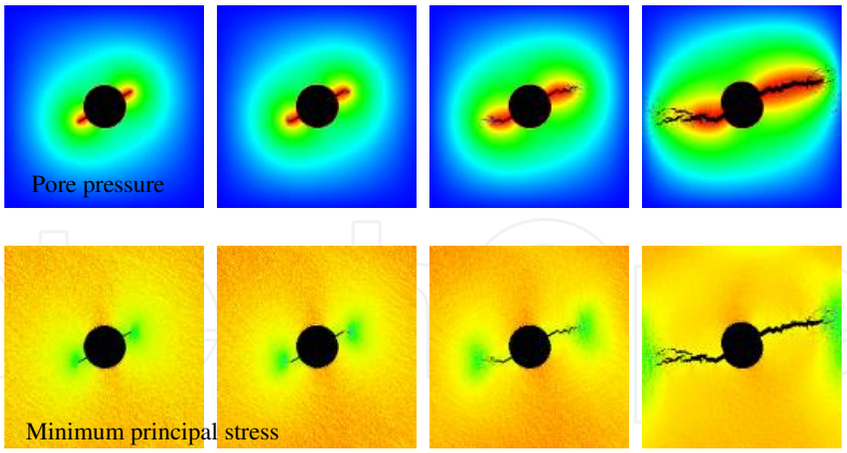

Figure 6. Pore pressure and the minimum principal stress distribution in fracture evolution process (30°)

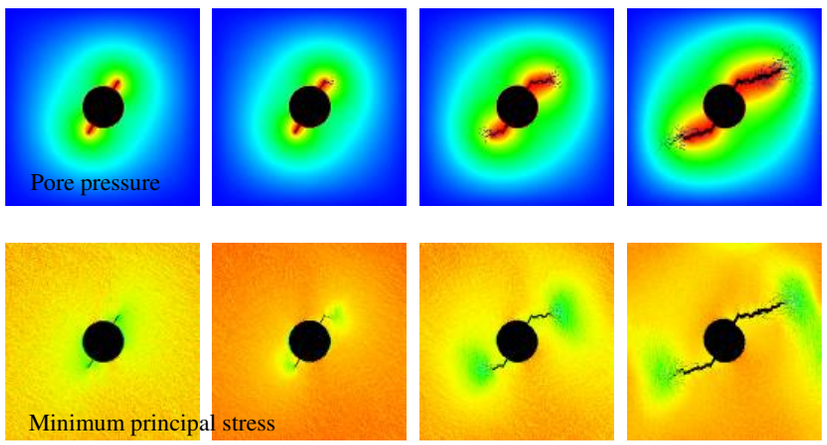

Figure 7. Pore pressure and the minimum principal stress distribution in fracture evolution process (45°)

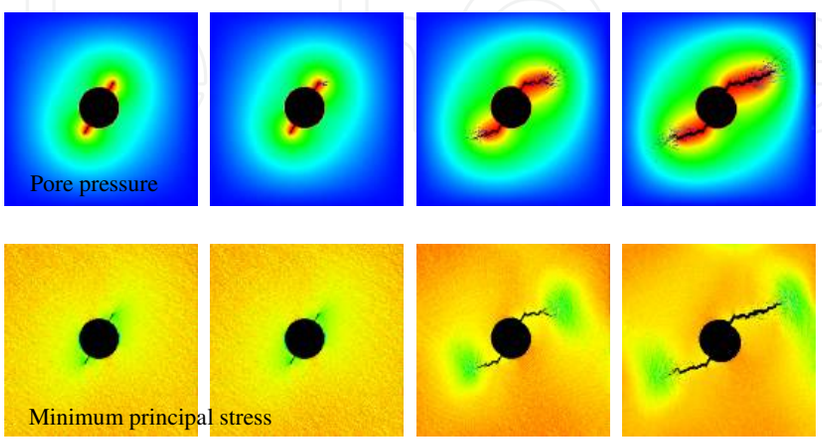

Figure 8. Pore pressure and the minimum principal stress distribution in fracture evolution process (60°)

http://dx.doi.org/10.5772/56012

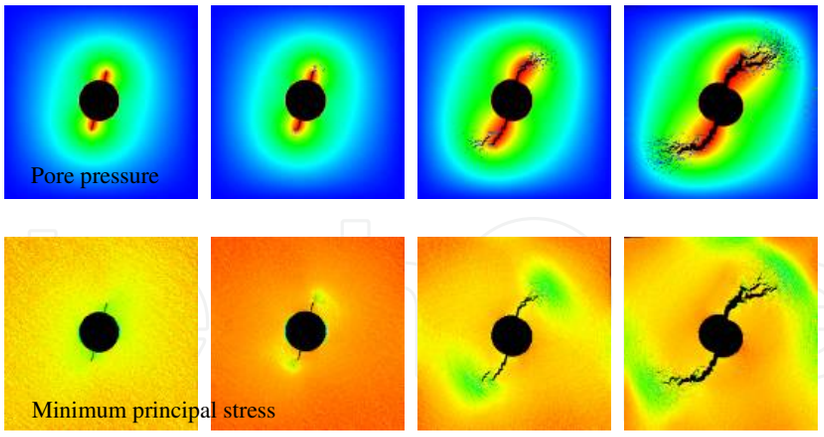

Figure 9. Pore pressure and the minimum principal stress distribution in fracture evolution process (75°)

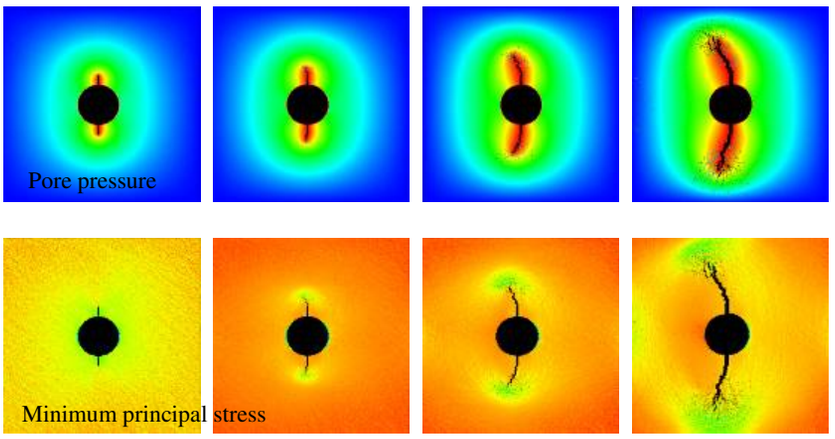

Figure 10. Pore pressure and the minimum principal stress distribution in fracture evolution process (90°)

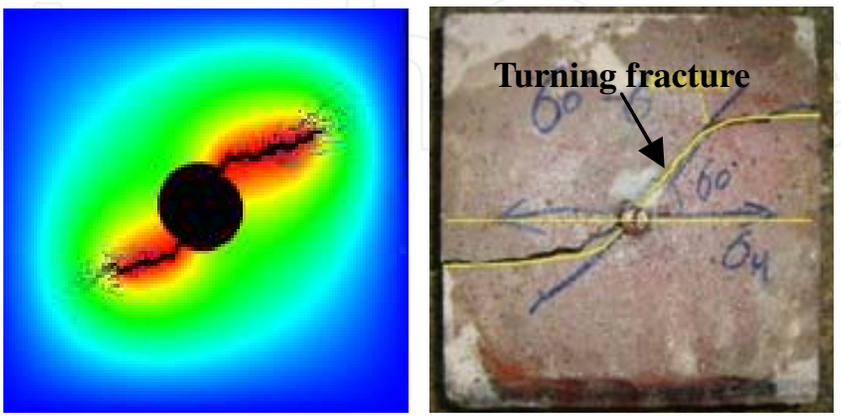

Figure 11. Comparison of numerical simulation and experimental results in [4] which has the same perforation angle (60°) and under the same ground stress difference (5MPa)

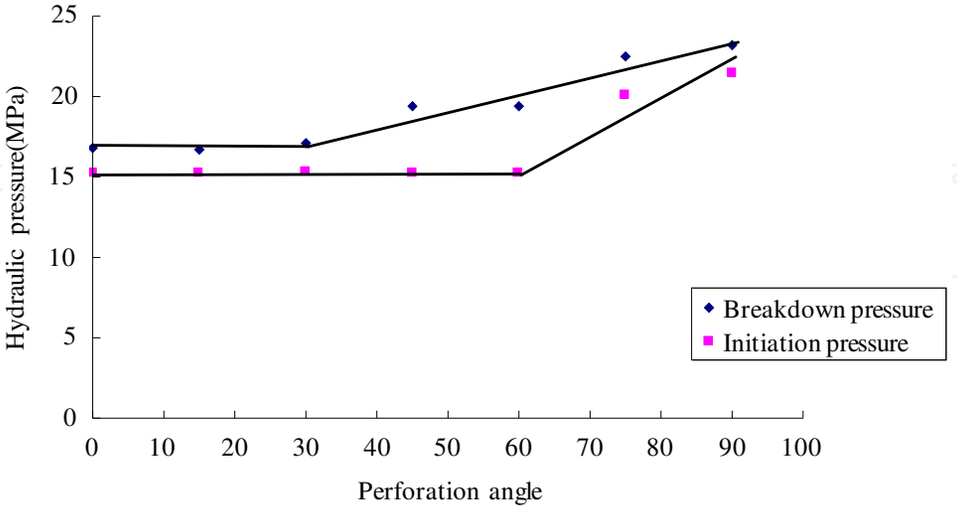

Figure 12. Changes of initiation and breakdown pressure of different perforation angle specimens

4.2. The effect of bedding angles

The initiation pressure, the breakdown pressure and the fracture evolution of seven rock specimens with different bedding angles are simulated. Pore pressure and the minimum principal stress distribution achieved by numerical simulation are shown from figure 13 to figure 19, and the values of initiation and breakdown pressure shown in figure 20.

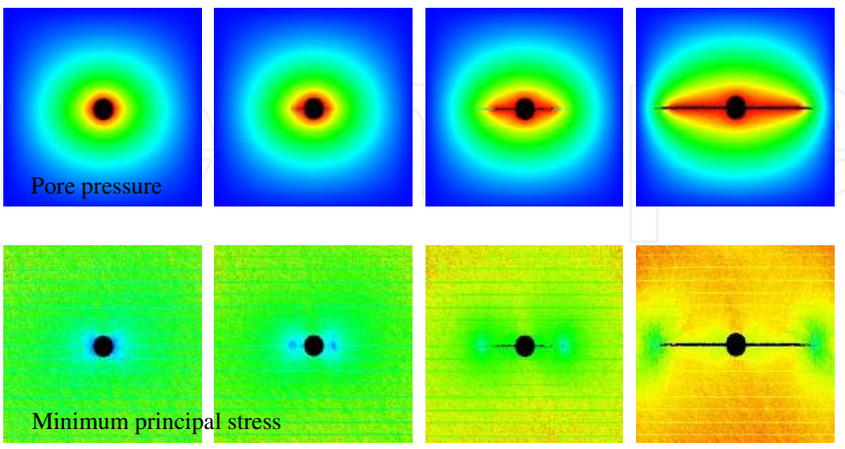

Figure 13. Pore pressure and the minimum principal stress distribution in fracture evolution process (0°)

http://dx.doi.org/10.5772/56012

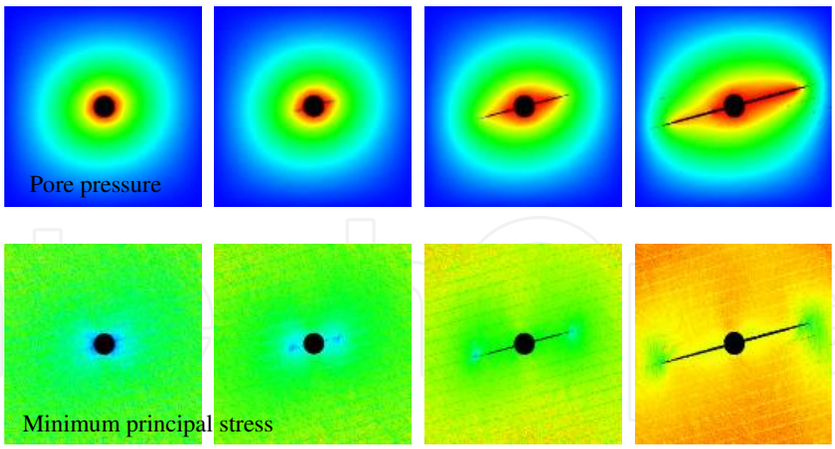

Figure 14. Pore pressure and the minimum principal stress distribution in fracture evolution process (15°)

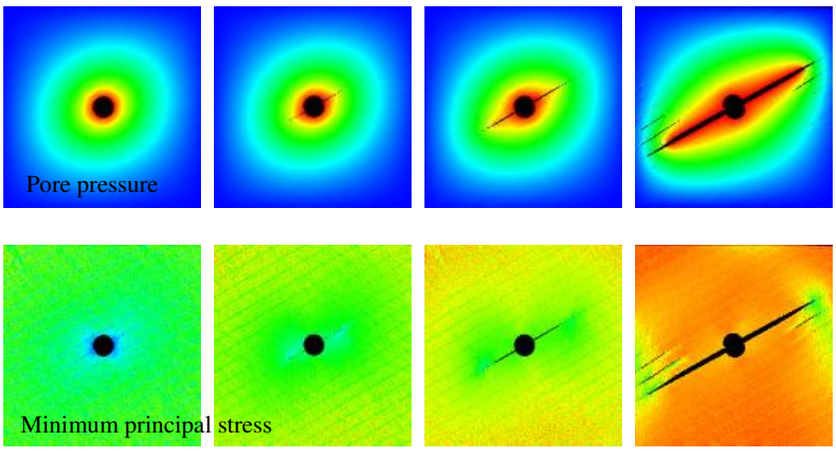

Figure 15. Pore pressure and the minimum principal stress distribution in fracture evolution process (30°)

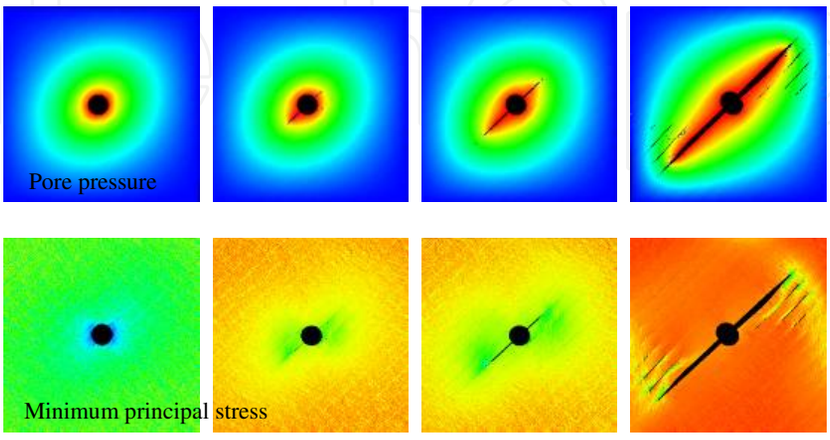

Figure 16. Pore pressure and the minimum principal stress distribution in fracture evolution process (45°)

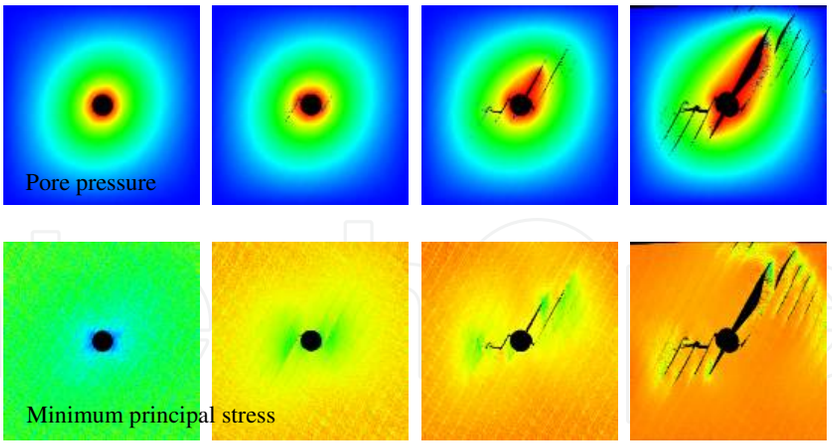

Figure 17. Pore pressure and the minimum principal stress distribution in fracture evolution process (60°)

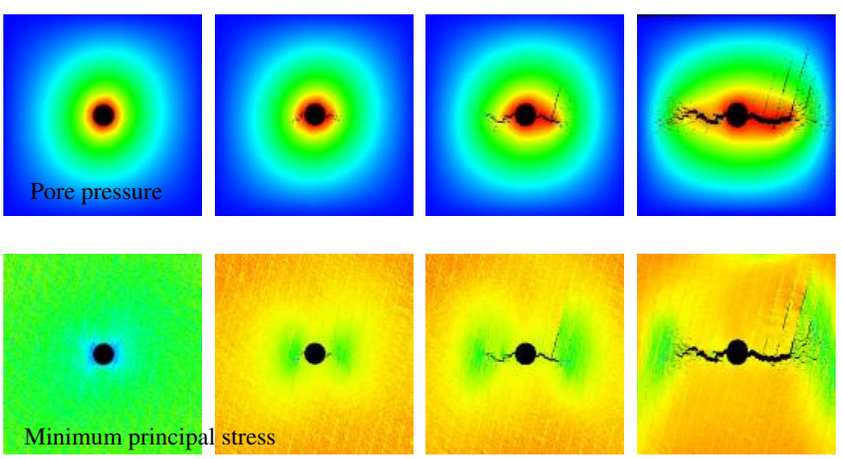

Figure 18. Pore pressure and the minimum principal stress distribution in fracture evolution process (75°)

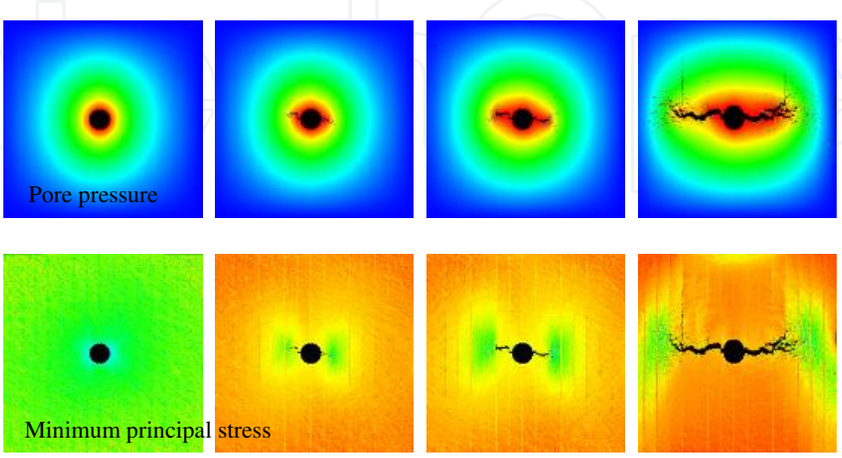

Figure 19. Pore pressure and the minimum principal stress distribution in fracture evolution process (90°)

http://dx.doi.org/10.5772/56012

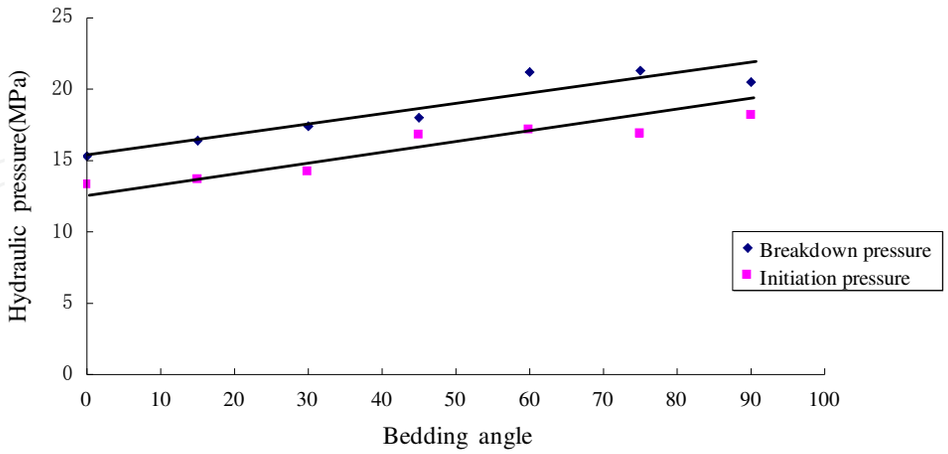

Figure 20. Changes of initiation and breakdown pressure of different bedding angle specimens

4.3. The effect of bedding materials

Taking the rock specimen of 60° bedding angle for example, the initiation pressure, the breakdown pressure and the fracture evolution of seven rock specimens with different bedding materials are simulated. Pore pressure and the minimum principal stress distribution achieved by numerical simulation are shown from figure 21 to figure 27 and the values of initiation and breakdown pressure shown in figure 28.

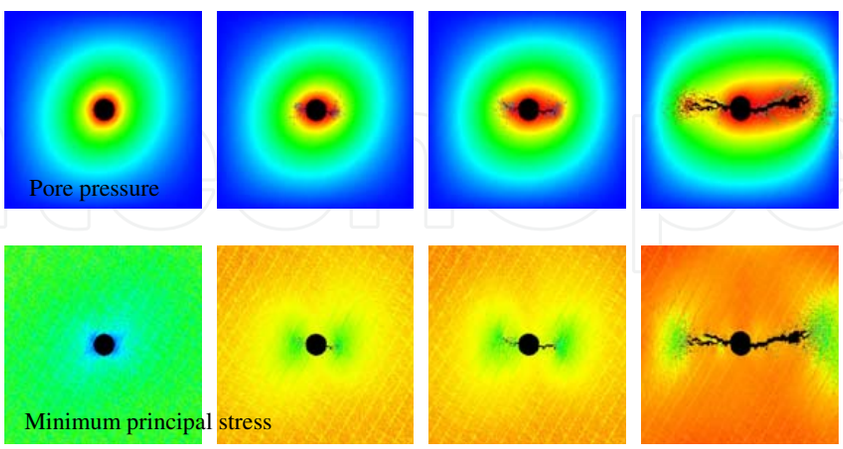

Figure 21. Pore pressure and the minimum principal stress distribution in fracture evolution process (elastic modulus value is 3.0GPa)

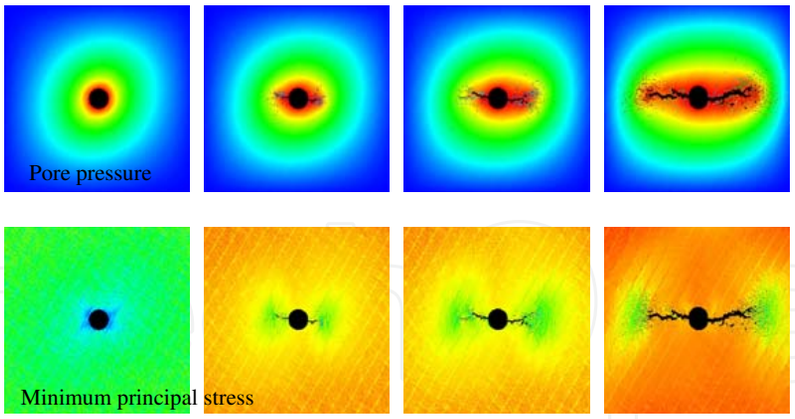

Figure 22. Pore pressure and the minimum principal stress distribution in fracture evolution process (elastic modulus value is 1.5GPa)

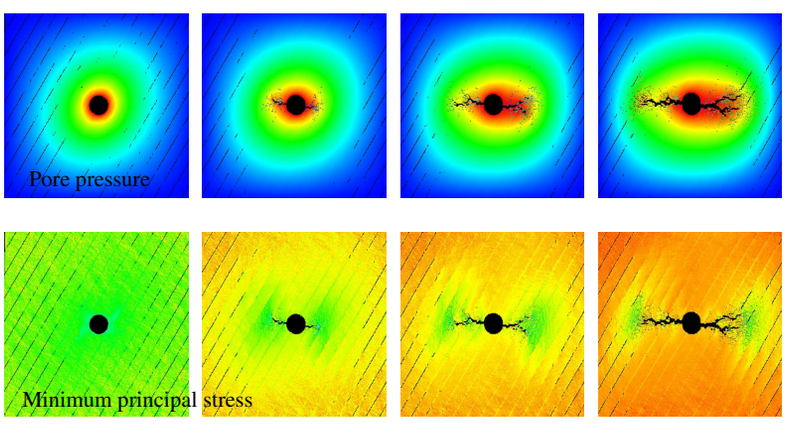

Figure 23. Pore pressure and the minimum principal stress distribution in fracture evolution process (elastic modulus value is 0.5GPa)

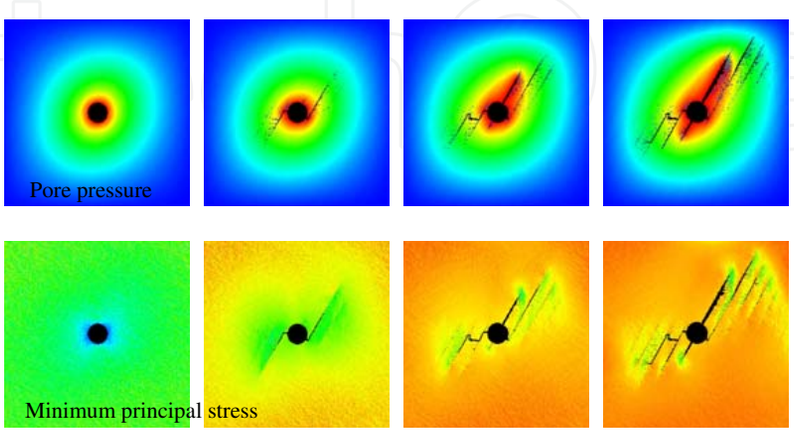

Figure 24. Pore pressure and the minimum principal stress distribution in fracture evolution process (uniaxial compressive strength value is 20MPa)

http://dx.doi.org/10.5772/56012

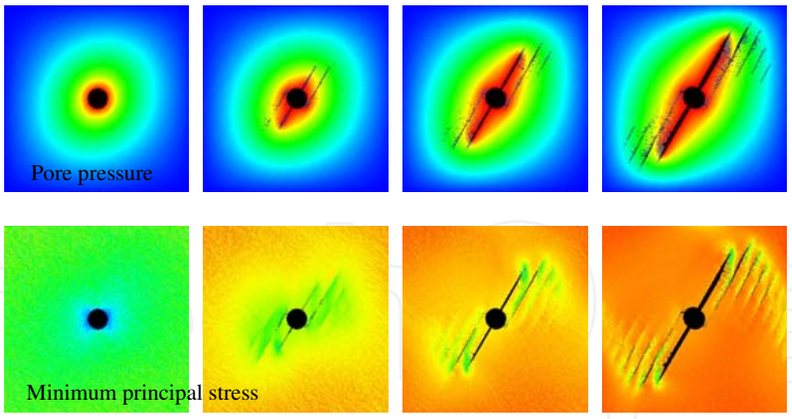

Figure 25. Pore pressure and the minimum principal stress distribution in fracture evolution process (uniaxial compressive strength value is 10MPa)

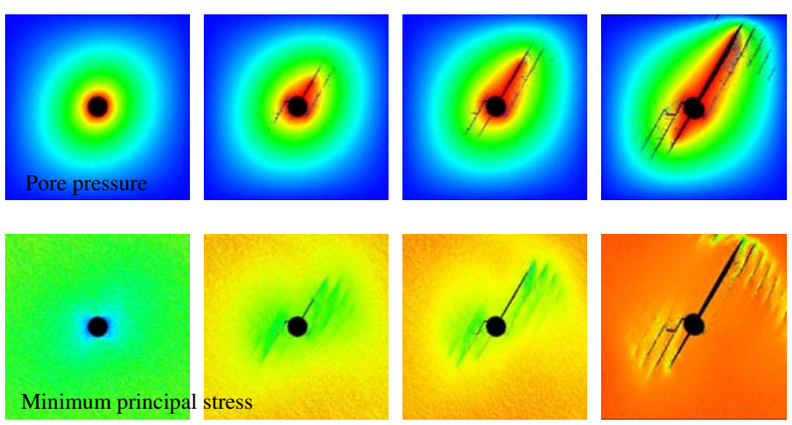

Figure 26. Pore pressure and the minimum principal stress distribution in fracture evolution process (uniaxial compressive strength value is 3.33MPa)

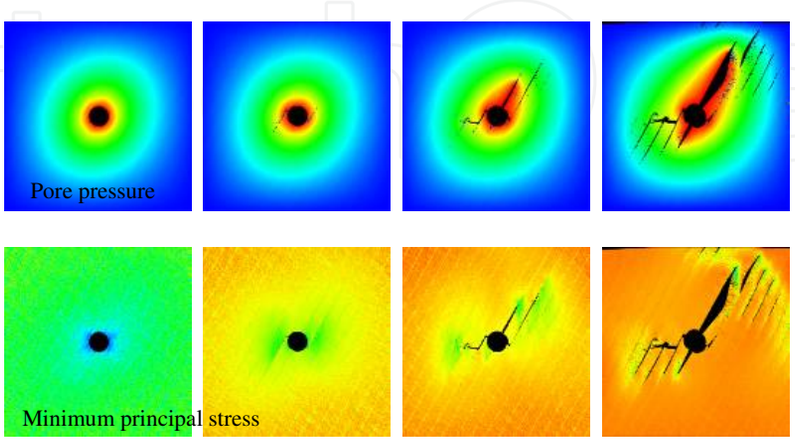

Figure 27. Pore pressure and the minimum principal stress distribution in fracture evolution process (elastic modulus value is 3.0GPa and uniaxial compressive strength value is 20MPa)

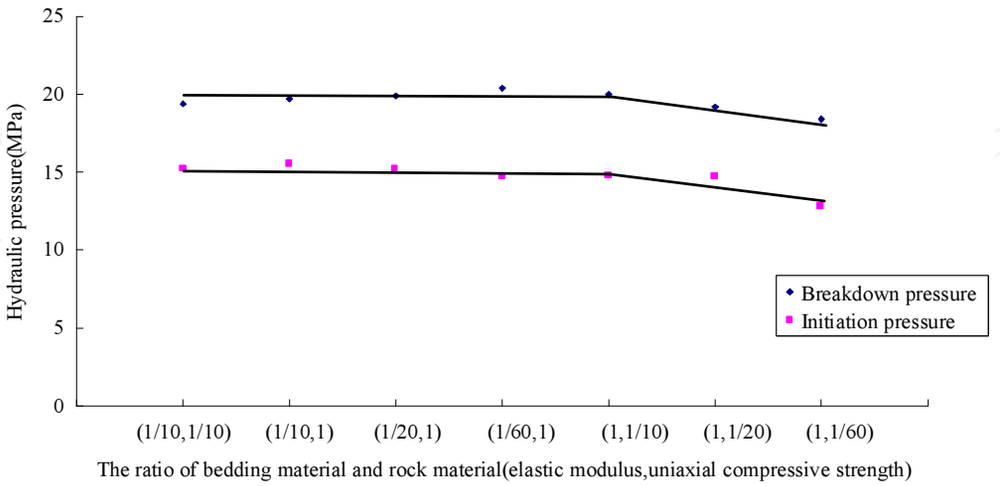

Figure 28. Changes of initiation and breakdown pressure of different bedding material specimens

5. Discussions

From the simulation results of the first group, we can see that the hydraulic fracturing process of the rock specimens with different perforation angle under constant confining pressure is divided into three stages:

1. Stress accumulation stage

In this stage, there doesn't appear any fracture and broken element, but as the pore pressure increases step by step, the stress is accumulating on perforation tip gradually and forming a high minimum principal stress area (green zone). Because of the tensile strength of rock is far less than the compressive strength, it can be speculated that the fracture initiation will be happened on the perforation tip where tensile stress is the largest;

2. Steady propagation stage

The fracture will initiate and propagate on perforation tip when the minimum principal stress accumulates to a certain point (tensile strength). In this stage, lots of micro fractures will appear on the main fracture tip as the loading step increases, and distributing as an umbrella and disconnected to each other;

3. Unsteady propagation stage

As the number of micro fractures increase, some micro fractures connect to each other and become secondary fractures. In this stage, in the process of fracture propagation, stress is

http://dx.doi.org/10.5772/56012

released from parts of the high stress area and transferred to the fracture tip, which makes the fracture propagate continually under the constant hydraulic pressure. The speed of fracture propagation become faster and faster and the main fracture and the secondary fractures are connected finally.

From figure 4 to figure 10, it can be concluded that no matter how the perforation azimuth changes, the fracture is still initiating on the perforation tip, which is because of the casing. But after the fracture initiate, the fracture propagation will turn to the horizontal direction (the maximum principal stress direction) gradually under the increasing hydraulic pressure and form a turning fracture finally. The perforation angle is bigger, the fracture turning will be more obvious and the turning distance will be bigger. Fracture propagation is always deviating from the perforation direction to the maximum principal stress direction (horizontal direction), which proves that the effect of perforation angle on the direction of fracture propagation is small and the maximum principal stress control the final fracture propagation direction.

The results also show that the perforation angle determines the initiation and the breakdown pressure of rock specimens. With the perforation angle increases, the initiation pressure are 15.2MPa, 15.2MPa, 15.3MPa, 15.2MPa, 15.2MPa, 20.1MPa and 21.4MPa respectively, and the breakdown pressure 16.8MPa, 16.7MPa, 17.1MPa, 19.4MPa, 19.4MPa, 22.5MPa and 23.2MPa respectively. The initiation pressure and the breakdown pressure are divided into two stages (figure 12): When $\alpha \leq 60^o$, the values of initiation pressure are small and basically constant, while as $\alpha > 60^o$, the values of initiation pressure increase obviously and with the increase of α, the values of initiation pressure will increase gradually; When $\alpha \leq 30^o$, the values of breakdown pressure are small and basically constant, while as $\alpha > 30^o$, the value of breakdown pressure will increase obviously and with the increase of α, the values of breakdown pressure will increase gradually, of which the increase rate is smaller than that of initiation pressure. Therefore, 0^o-30^o is the best perforation azimuth area and the values of initiation and breakdown pressure are small, which may help reduce fracturing cost and improve the fracturing efficiency. The comparison of numerical simulation results and the experimental results with the same perforation angle (60^o) and ground stress difference (5MPa) is shown in figure 11 and we can find that the macroscopic fracture propagation of the numerical simulation is basically consistent with the experimental results.

The results of first group simulation indicates that the maximum principal stress determines the fracture propagation direction, and the effect of bedding angles of rock specimens under the same confining pressure on fracture propagation will be studied in the second group.

From the simulation results of the second group, we can conclude that the fracture initiation and the propagation pattern of rock specimens under constant confining pressure are changing gradually as bedding angle increases. From figure 13 to figure 19, we can see that, when bedding angle α is small (0^o~15^o), the initiation and propagation of fracture are only along with the tension failure bedding. Because of the stress accumulation, there exist a high tensile stress area on the fracture tip and because the bedding material is weaker than rock ma-

terial, the fracture propagation is along the cracked bedding and form a straight fracture eventually. In this case, the bedding plane determines the fracture evolution.

When bedding angle α increases slightly (30°~45°), the initiation and propagation of fracture is still along the tension failure bedding. With the increase of loading step, there is a high tensile stress area on the main fracture tip which is along the cracked bedding and the beddings in the high tensile stress area are cracked and form secondary fractures paralleling to the main fracture, moreover, with the increase of bedding angle, the number of secondary fractures is increasing gradually. Because of the advantage of main fracture, the fracture propagation is still along the main fracture bedding.

When the bedding angle α continues to increase (60°), the fracture will turn from along the tension failure bedding to the horizontal direction that is the main fracture and the secondary fractures paralleling to the main fracture is still initiating and propagating in bedding plane with the horizontal secondary fracture initiating at the same time and connecting the main fracture and the parallel secondary fractures gradually. In this case, the bedding plane and the maximum principal stress determine the fracture evolution together.

When bedding angle α is big (75°~90°), the initiation and propagation of fracture is no longer along the bedding plane. Because of the heterogeneous characteristics of rock and bedding materials, different strength elements are in random distribution causing an uneven stress distribution and the local stress concentration thus making the fracture become bend and rough, but the general trend is the maximum principal stress direction. In this case, the effect of bedding plane on fracture evolution is almost disappeared, but the maximum principal stress controls the fracture initiation and propagation. Comparing figure 4 and figure 19, we can find that the existence of bedding influences the fracture shape greatly in the same condition as the maximum principal stress controls the fracture evolution.

From the numerical simulation results, as bedding angle increase, the values of initiation pressure are 13.3MPa, 13.7MPa, 14.2MPa, 16.8MPa, 17.1MPa, 16.9MPa and 18.2MPa respectively, and the values of breakdown pressure 15.3MPa, 16.4MPa, 17.4MPa, 18MPa, 21.2MPa, 21.3MPa and 20.5MPa respectively. Both of the values of initiation and breakdown pressure are in a linear growth (figure 20) with the growth rate similar and as the bedding plane is parallel to the maximum principal stress direction (bedding angle is 0°), the specimen is in the most unstable situation.

Because the fracture propagation is determined by the maximum principal stress and the bedding plane together when bedding angle is 60° seeing from the second group simulation, taking the bedding angle of 60° for example, in the third group, the effect of strength and stiffness of bedding material on fracture evolution will be studied under the combined effects of the maximum principal stress and the bedding plane.

In the third group, the rock specimens with the same bedding angle but different materials are under the constant confining and increasing hydraulic pressure. As the strength of bedding material is constant (bedding strength/rock strength is 1), but the stiffness decreased

http://dx.doi.org/10.5772/56012

(bedding elastic modulus/rock elastic modulus is 1/10, 1/20, 1/60), the pattern of fracture propagation will be unchanged. Because of the reduction of elastic modulus, the initiation pressure reduced (15.5 MPa, 15.2 MPa, 14.7 MPa) and the breakdown pressure increased slightly (19.7 MPa, 19.9 MPa, 20.4 MPa), however, both of the reduction and the increase can be ignored because the values of the initiation and the breakdown pressure are almost constant (figure 28). As the stiffness of the bedding material (bedding elastic modulus/rock elastic modulus is 1) is constant but the strength decreased (bedding strength/rock strength is 1/10, 1/20, 1/60), the pattern of the fracture propagation will be unchanged, and the values of initiation (14.8 MPa, 14.7 MPa, 12.8 MPa) and breakdown pressure (20 MPa, 19.2 MPa, 18.4 MPa) decreased gradually with almost the same decrease rates (figure 28). As both of the stiffness and strength are decreased (bedding elastic modulus/rock elastic modulus is 1/10, bedding strength/rock strength is 1/10), the initiation pressure, the breakdown pressure and the pattern of fracture propagation are almost the same as the condition of (1, 1/10). As suggested above, the stiffness of bedding material has little influence on initiation pressure, breakdown pressure and fracture evolution of rock specimens, except that the strength determines them.

In summary, the damage process of rock specimen are determined by the maximum principal stress, the bedding angle and the strength of bedding material, while the effect of perforation angle and stiffness is small and can be ignored.

6. Conclusions

Based on the simulation results of three groups, the following can be concluded:

1. When perforation angle is larger than 0^o, a turning fracture will be formed, and if the perforation angle turns bigger, the fracture turning will be more obvious and the turning distance bigger. The effect of perforation angle on fracture propagation direction is small, and the maximum principal stress controls the fracture propagation direction.
2. The initiation and the breakdown pressure of specimens with different perforation angles are divided into two stages and 0^o-30^o is the best perforation angle area. The initiation and the breakdown pressure can be predicted through the numerical simulation.
3. The influence of bedding angle on initiation pressure, breakdown pressure, fracture shape and fracture propagation pattern is great. As the bedding angle increases, the bedding plane and the maximum principal stress will control the fracture evolution respectively and the initiation and the breakdown pressure are in a linear growth with the similar rates. The specimen will be in the most unstable situation as the bedding plane paralleling to the maximum principal stress direction.
4. The stiffness of bedding material has little influence on damage process of rock specimens, except that the strength controls it. With the decrease of bedding material strength, the initiation and the breakdown pressure will decrease gradually with the similar decrease rates.

Author details

Xiaoxi Men[1*], Chun'an Tang[2], Shanyong Wang[3], Yongping Li[4], Tao Yang[2] and Tianhui Ma[2]

*Address all correspondence to: menxiaoxi@126.com; tang_chunan@yahoo.com; Shanyong.Wang@newcastle.edu.au; liyp69@petrochina.com.cn; 361721644@qq.com; 19928600@qq.com

1 Northeastern University, Shenyang, China

2 Dalian University of technology, Dalian, China

3 ARC Centre for Geotechnical Science and Engineering, The University of Newcastle, NSW, Australia

4 Fracturing and Acidizing Technical Service Center, Research Institute of Petroleum Exploration & Development-Langfang, Petrochina, Langfang, China

References

[1] Daneshy, Abbas Ali, Halliburton Services. Experimental Investigation of Hydraulic Fracturing Through Perforations. Petroleum Technology (1973). , 25(10), 1201-1206.

[2] Weng, X W. Fracture Initiation and Propagation from Deviated Wellbores. In: Proceedings of the SPE Annual Technical Conference and Exhibition, Houston, Texas, 30 Oct (1993). Paper SPE 26597.

[3] Zhang, X, Jeffrey, R G, Bunger, A P, & Thiercelin, M. Initiation and Growth of a Hydraulic Fracture from a Circular Wellbore. Rock Mechanics and Mining Sciences (2011).

[4] Zhang, G Q, Chen, M, Wang, X S, & Zhao, C. Influence of Perforation on Formation Fracturing Pressure. Petroleum Science (2004). , 1(3), 56-61.

[5] Jiang, H, & Chen, M. Impact of Oriented Perforation on Hydraulic Fracture Initiation and Propagation. Chinese Journal of Rock Mechanics and Engineering (2009). , 28(7), 1321-1326.

[6] Brouno, M S, & Nakagawa, F M. Pore Pressure Influence on Tensile Fracture Propagation in Sedimentary Rock. International Journal of Rock Mechanics and Mining Science & Geomechanics Abstracts (1991). , 28(4), 261-273.

[7] Li, L C, & Tang, C A. Simulation of Multiple Hydraulic Fracturing in Non-uniform Pore Pressure Filed. Advanced Materials Research (2005). , 9, 163-172.

[8] Abbass, T, & André, V. Effect of Layer Orientation on the Failure of Layered Sandstone under Brazilian Test Conditions. International Journal of Rock Mechanics and Mining Sciences (2010). , 47(2), 313-322.

[9] Abbass, T. Failure of Layered Sandstone under Brazilian Test Conditions: Effect of Micro-scale Parameters on Macro-scale Behaviour. Rock Mechanics and Rock Engineering (2010). , 43(5), 641-653.

[10] Tang, C A, Tham, L G, Lee, P, Yang, K, & Li, T H. L C. Coupled Analysis of Flow, Stress and Damage (FSD) in Rock Failure. International Journal of Rock Mechanics & Mining Sciences (2002). , 39(4), 477-489.

[11] Leng, X F, & Yang, T H. Numerical Simulation and Analysis of Rocks with Single Hole Each Under Hydraulic Fracturing. World Nonferrous Metals (2002). , 10, 32-34.

[12] Tang, C A. Numerical Simulation to Influence of Pore Pressure Magnitude and Gradient on Fracture Propagation in Brittle Heterogeneous Rocks. Rock and Soil Mechanics (2003). , 24, 17-20.

[13] Yang, T H. Influence of Heterogeneity of Mechanical Properties on Hydraulic Fracturing in Permeable Rocks. Rock Mechanics and Rock Engineering (2004). , 37(4), 251-275.

[14] Li, G, & Tang, C A. Three-Dimensional Micro Flow-Stress-Damage (FSD) Model and Application in Hydraulic Fracturing in Brittle and Heterogeneous Rocks. Key Engineering Materials (2011).

[15] Yang, T H. Numerical Approach to Hydraulic Fracturing in Heterogeneous and Permeable Rocks. Key Engineering Materials (2003).

[16] Yang, T H, & Tang, C A. Numerical Simulation of Hydraulic Fracturing Process in Heterogeneous Rocks under Different Confining Pressures. Chinese of Computational Mechanics (2004). , 21(4), 419-424.

IntechOpen